Civil Engineering Beyond Limits 2 (2027) 11196
Civil Engineering Beyond Limits
journal home: www.acapublishing.com/journals/1/cebel

Research Article

Temporal, Spatial, and Depth-Dependent Seismicity of Takhar, Afghanistan: Insights from b-Value Variations and Seismic Moment Release

Hedayatullah Hawadi*,[1]
[1]Department of Geophysics, Faculty of Nano and Bio Science and Technology, Persian Gulf University, Bushehr, Iran

Keywords

Gutenberg–Richter relationship,
b-value,
Temporal variation,
Spatial distribution,
Takhar,
Hindu Kush–Pamir.

Abstract

Understanding the temporal, spatial, and depth-dependent characteristics of seismicity is essential for evaluating earthquake processes and seismic hazard in tectonically complex regions. This study investigates the seismicity of Takhar Province and its surrounding region, Afghanistan, using a catalogue of 5,076 earthquakes recorded between 1926 and 2025. The earthquake catalogue was processed by removing duplicate and incomplete records and homogenizing magnitude information to moment magnitude (Mw). The Gutenberg–Richter relationship was applied to characterize earthquake-size distributions and variations in the b-value across temporal, spatial, and depth domains. The overall b-value was estimated at 1.18 ± 0.02, with a magnitude of completeness (Mc) of approximately 4.6. Spatial analysis revealed substantial heterogeneity, with b-values ranging from approximately 0.8 to 2.2 and relatively low values concentrated in several parts of Takhar. Temporal analysis showed a distinctly non-uniform pattern, characterized by relatively quiet intervals interrupted by episodes of enhanced seismic activity. Temporal b-values also varied among major seismic sequences. Cumulative seismic moment revealed abrupt increases associated with major earthquakes, reflecting episodes of rapid seismic moment release. Depth-dependent variations in b-value demonstrated significant vertical heterogeneity in seismic deformation. Overall, the results indicate that Takhar exhibits a complex and heterogeneous seismic regime across time, space, and depth within the broader Hindu Kush–Pamir tectonic system. The findings provide useful statistical constraints for understanding earthquake-generating processes and improving regional seismic-hazard assessment.

1. Introduction

Earthquakes result from the sudden release of accumulated strain and stress within the Earth's crust and lithosphere [1]. Their spatial, temporal, and frequency–magnitude distributions provide valuable information about the mechanical, structural, and tectonic characteristics of seismically active regions. The Gutenberg–Richter (G–R) relationship is a fundamental statistical framework for describing the frequency–magnitude distribution of earthquakes and the relative proportion of small- and large-magnitude events[2, 3]. In combination with analyses of earthquake clustering, focal depth, and cumulative seismic moment release, the frequency–magnitude distribution provides important constraints on regional seismic behavior and seismic hazard [4].

The Hindu Kush–Pamir region forms part of the India–Eurasia continental collision zone and represents one of the most complex active deformational systems in continental Asia [5–8]. Regional deformation is accommodated by interacting thrust, strike-slip, and other fault systems, while the Hindu Kush is characterized by an exceptional concentration of intermediate-depth earthquakes extending to several hundred kilometers beneath the region [9–11]. The coexistence of shallow crustal and intermediate-depth seismicity provides an important natural setting for investigating the relationships among tectonic structure, focal depth, and earthquake frequency–magnitude characteristics [12].

Takhar Province, located in northeastern Afghanistan, lies within the southern Pamir–Hindu Kush tectonic system and is affected by a complex network of active and potentially active faults [5, 13]. Important structures in and around the study area include segments of the Central Badakhshan Fault Zone (CBF) with a mapped extent of approximately 280 km and an assigned slip rate of approximately 12 mm/yr, and the Darvaz fault (Df) with a mapped extent of approximately 300 km and an assigned slip rate of approximately 7 mm/yr, together with associated thrust and strike-slip structures (Figure 1a). These tectonic structures contribute to regional deformation and may influence the spatial distribution of seismicity [14, 15]. The Darvaz fault system represents an important strike-slip boundary along the western Pamir [13], while the relationship between these structures and the intermediate-depth Hindu Kush seismic zone provides a useful framework for investigating variations in earthquake occurrence with location and focal depth. The destructive 1998 earthquake sequence in the Rustaq area further demonstrates the significant seismic hazard of northeastern Afghanistan [16, 17].

The Gutenberg–Richter b-value, which describes the relative proportion of small to large earthquakes, is an important parameter for characterizing earthquake populations. Spatial and temporal variations in b-value have been associated with differences in tectonic setting, faulting conditions, structural heterogeneity, and differential stress [18–20]. In particular, lower b-values have often been associated with relatively higher differential stress in some tectonic environments [3]. However, b-value is not a direct measurement of stress and can also be strongly affected by earthquake-catalogue completeness, magnitude uncertainty, earthquake clustering, spatial sampling, and the statistical

*Corresponding Author: Hedayat.Hawadi@mehr.pgu.ac.ir, hidayatullahhawadi371@gmail.com
Received 14 Sep 2026; Revised 20 Oct 2026; Accepted 27 Oct 2026
https://doi.org/10.36937/cebel.2027.11196
2687-5756 /© 2022 The Authors, Published by ACA Publishing; a trademark of ACADEMY Ltd. All rights reserved.

estimation method [21–23]. Therefore, variations in b-value should be interpreted as statistical characteristics of seismicity and considered together with independent geological and seismological evidence [24].

Previous studies in the Hindu Kush, Pamir, and northwestern Himalaya have documented substantial spatial and depth-dependent variations in b-value and have identified differences between shallow and intermediate-depth earthquake populations [25–27]. Rehman et al. (2017), for example, reported differences in b-values between shallow and intermediate-depth seismicity in the Hindu Kush, while other studies have demonstrated significant heterogeneity in b-value across the broader Pamir–Hindu Kush region. However, direct comparison among these studies is complicated by differences in catalogue duration, magnitude scales, completeness thresholds, spatial coverage, depth ranges, and statistical procedures. Moreover, most previous investigations have considered relatively broad regional domains, and the long-term statistical characteristics of seismicity in Takhar Province remain comparatively poorly constrained.

Another important aspect of regional seismicity is cumulative seismic moment release. Because seismic moment increases strongly with earthquake magnitude, a relatively small number of large earthquakes can account for a substantial proportion of the total seismic moment released over a given period (Hanks and Kanamori, 1979) [28]. Consequently, combining b-value analysis with cumulative seismic moment provides complementary information: b-value describes the relative distribution of earthquake sizes, whereas seismic moment quantifies the contribution of earthquakes to the overall deformation and energy-release process.

The present study addresses this gap by analyzing a homogenized catalogue of 5,076 earthquakes recorded between 1926 and 2025 in Takhar Province and the surrounding region. The objectives are to: (1) characterize the regional frequency–magnitude distribution and estimate the magnitude of completeness; (2) determine the overall Gutenberg–Richter b-value; (3) investigate spatial and temporal variations in b-value; (4) examine the relationship between b-value and focal depth; and (5) quantify the cumulative seismic moment release associated with major earthquakes. By integrating frequency–magnitude analysis, spatial and temporal b-value distributions, focal-depth information, and cumulative seismic moment, this study provides a comprehensive statistical characterization of seismicity in Takhar Province and contributes to a better understanding of its relationship with the complex tectonic processes of the Hindu Kush–Pamir collision zone.

1.1. Gutenberg–Richter Law and b-Value

The Gutenberg–Richter (G–R) relationship is one of the most widely used empirical laws for describing the frequency–magnitude distribution of earthquakes. It expresses the relationship between earthquake magnitude and the cumulative number of events exceeding a given magnitude as [29]:

$$log_{10}N = a - bM \tag{1}$$

where N represents the cumulative number of earthquakes with a magnitude equal to or greater than M. The constants a and b characterize different aspects of regional seismicity. The a-value is generally considered an indicator of the overall level of seismic activity, with higher values corresponding to greater earthquake occurrence rates. In contrast, the b-value describes the relative proportion of small- and large-magnitude earthquakes and is therefore an important parameter for characterizing the frequency–magnitude behavior of a seismic region[2, 3, 30].

Spatial and temporal variations in the b-value have been widely investigated as indicators of changes in the physical and tectonic conditions of the Earth's crust [31]. In particular, the b-value is often associated with the stress state of a seismogenic region and may be influenced by factors such as fault frictional properties and tectonic boundary conditions, including those associated with subduction processes [32]. Numerous studies have reported an inverse relationship between differential stress and the b-value, suggesting that a reduction in b-value may be associated with increasing stress accumulation during certain stages of the seismic cycle [24].

Variations in b-value may also reflect differences in fault behavior and structural heterogeneity. Fault segments characterized by stable or creeping deformation are commonly associated with relatively high b-values, whereas strongly coupled asperities, where stress may accumulate, often exhibit lower values [29]. The spatial arrangement and connectivity of asperities can further influence the observed b-value distribution. In addition, crustal material heterogeneity and variations in thermal conditions have been identified as important factors affecting b-value estimates. An increase in structural heterogeneity and thermal gradients may contribute to elevated b-values, highlighting the complex relationship between seismicity statistics and the physical properties of the crust [8, 27, 33, 34].

This relationship provides an important statistical framework for investigating the temporal and spatial evolution of seismicity in Takhar Province. Analysis of variations in the Gutenberg–Richter parameters, particularly the b-value, can therefore contribute to a better understanding of regional stress conditions, fault behavior, and the processes controlling earthquake occurrence.

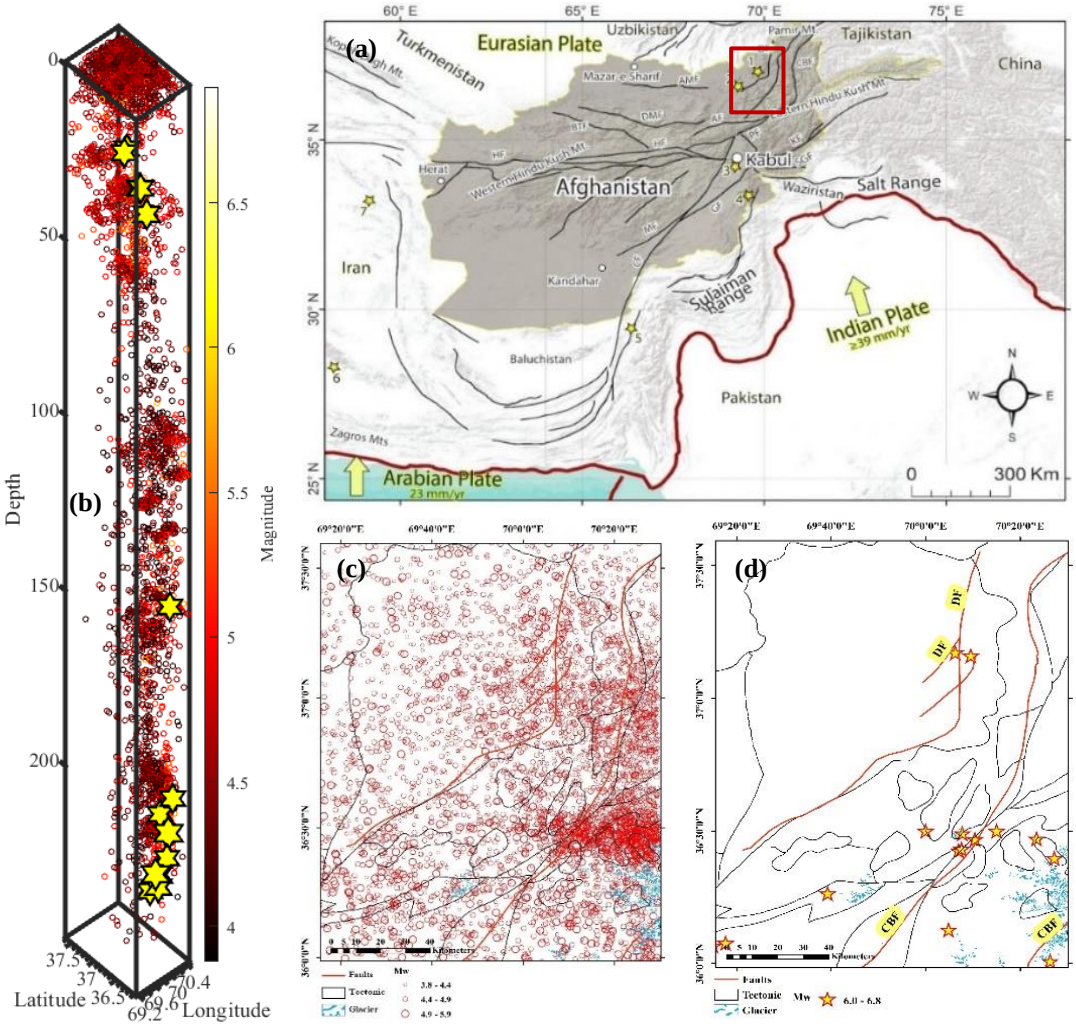


Figure 1. Seismotectonic setting and distribution of seismicity in Takhar Province, northeastern Afghanistan. (a) Location of Takhar Province in Afghanistan; (b) three-dimensional distribution of earthquake hypocenters; (c) spatial distribution of seismicity and major faults; and (d) enlarged view of the study area showing earthquakes with M ≥ 6.0 (stars).

2. Data and Methods

An earthquake catalogue was compiled from earthquake records obtained from the (ISC[1] Event catalogue) and (USGS[2] Search Earthquake Catalog)[35, 36]. The study area is geographically bounded by longitudes 69.18°E - 70.50° E, and latitudes 35.17° N - 37.60° N. For the spatial analysis, the study area was divided into a regular grid comprising 925 square cells, each measuring (5.8km×5.8km).

The parameters were calculated for each grid cell. The catalogue covers the period from 1926 to 2025 and contains information on earthquake origin time, geographic coordinates, focal depth, and magnitude Figure 2(b) and Figure 2(c). The records from the two catalogues were integrated and examined to identify duplicate and incomplete events. Duplicate and incomplete records were removed to minimize bias and redundancy in the dataset. After catalogue screening and quality control, 5,076 earthquake events were retained for the statistical analysis. The resulting catalogue was subsequently used to investigate the frequency–magnitude distribution, spatial and temporal variations in seismicity, depth-dependent b-value variations, and cumulative seismic moment release in the study region. Because the earthquakes in the original catalogue were reported using different magnitude scales, including surface-wave magnitude (Ms), body-wave magnitude (mb), and local magnitude (ML), the magnitudes were homogenized to moment magnitude (Mw) prior to the statistical analysis [25, 37]. The conversion relationships were applied according to the reported magnitude type and the corresponding magnitude range. For surface-wave magnitude, the following relationships were used:

$$Ms: Mw = 0.67(\pm 0.005)\, Ms + 2.07(\pm 0.03) \quad \text{for } 3.0 \le Ms \le 6.1$$

$$Ms: Mw = 0.99(\pm 0.020)\, Ms + 0.08(\pm 0.13) \quad \text{for } 6.2 \le Ms \le 8.2$$

For body-wave magnitude, the conversion relationship was

$$mb: Mw = 0.85(\pm 0.040)\, mb + 1.03(\pm 0.23) \quad \text{for } 3.5 \le mb \le 6.2$$

[1] International Seismological Centre
[2] United States Geological Survey

whereas local magnitude was converted using

$$\text{ML: } Mw = 0.934(\pm 0.135)\,ML + 0.356(\pm 0.714) \qquad \text{for } 3.4 \le ML \le 7.6$$

These relationships were used to establish a common magnitude scale for the earthquake catalogue and to reduce potential systematic effects associated with combining different magnitude scales. The uncertainties associated with the empirical conversion relationships were retained as reported with the corresponding equations.

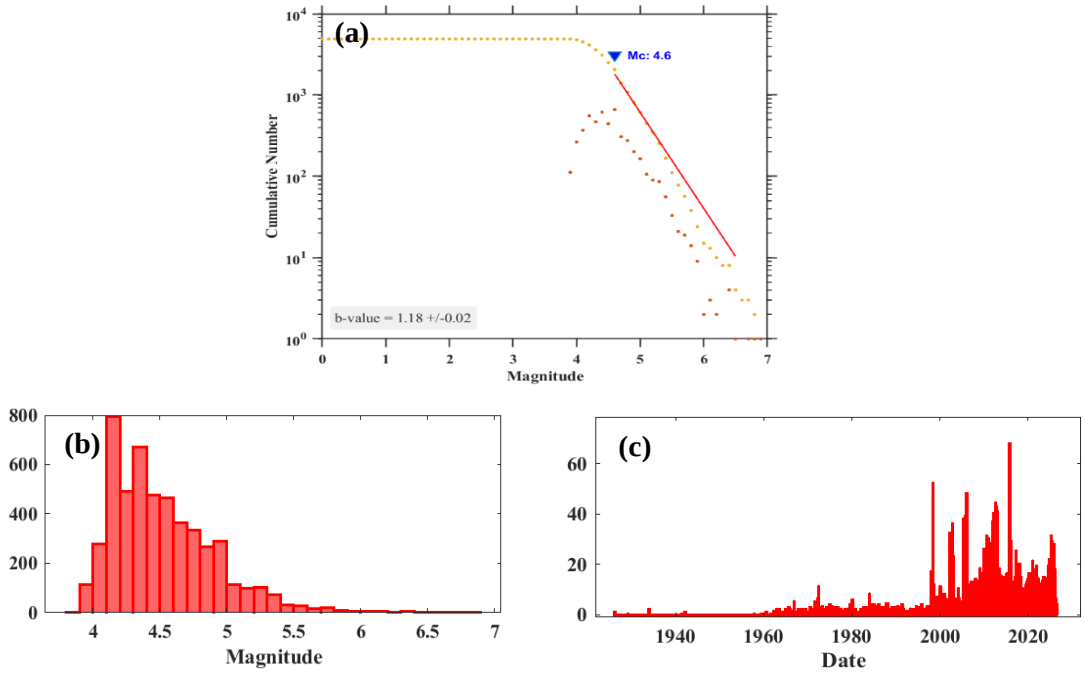


Figure 2. (a) Frequency distribution of declustered earthquakes in the Takhar region, northeastern Afghanistan, during 1926–2025; (b) earthquake frequency histogram; and (c) temporal distribution of earthquakes during 1926–2025, illustrating variations in seismic activity.

The magnitude of completeness (Mc) was estimated using the Maximum Curvature Method (MAXC) implemented in ZMAP7 running under MATLAB R2022b[38, 39]. The magnitude of completeness represents the lowest magnitude above which the earthquake catalogue is considered sufficiently complete for frequency–magnitude analysis [18]. Earthquakes with magnitudes below the estimated completeness threshold were excluded from the corresponding statistical analyses. The temporal analysis of catalogue completeness indicates that Mc was approximately 5.0–5.1 during the period from 1926 to 1995. After 2000 Figure 3, the estimated completeness magnitude generally decreased and showed greater temporal variability, which is interpreted as being associated with improvements in seismic monitoring and the increased detection capability for smaller earthquakes. An overall magnitude of completeness of approximately Mc = 4.6 Figure 2(a) was obtained for the study catalogue. The estimated temporal variations in completeness magnitude were considered when defining the earthquake population used for the frequency–magnitude and b-value analyses [32].

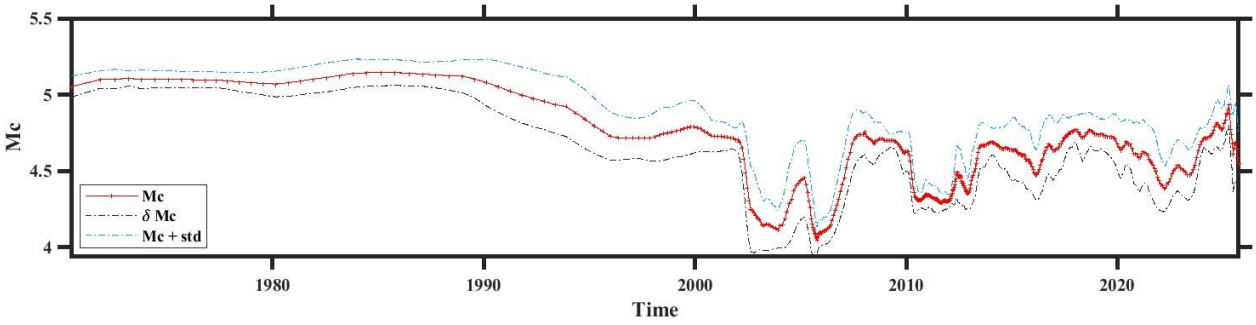


Figure 3. Temporal variation of the magnitude of completeness (M_c)

To reduce the influence of temporally and spatially clustered earthquakes, the earthquake catalogue was declustered using the Reasenberg algorithm(1985) [40, 41]. This method identifies earthquakes that are considered to be spatially and temporally associated and separates clustered events from independent seismicity on the basis of magnitude-dependent time and spatial interaction windows [42]. The following Reasenberg parameters were used: minimum look-ahead time τmin = 1 day, maximum look-ahead time τmax = 10 days, probability of detecting the next clustered event P1 = 0.95, interaction radius factor (xk) = 0.5, effective lower magnitude cutoff (xmeff) = 1.5, and the number of crack radii rfact = 10. The declustering procedure was applied to reduce the influence of dependent earthquake sequences, particularly aftershock sequences, on the statistical characterization of the regional earthquake population. The resulting independent-event catalogue was then used where required for statistical analyses of background seismicity [43, 44].

The b-value was estimated using the Maximum Likelihood Method because this approach provides a statistically robust estimate of the frequency–magnitude slope for earthquake populations above the magnitude of completeness [45].For earthquakes above the completeness threshold, the b-value was calculated as[42, 46]:

$$b = \frac{1}{\overline{M} - M_{min}} \log e \tag{2}$$

where $\overline{M}$ is the mean magnitude of the earthquakes included in the calculation and M_{min} is the effective minimum magnitude. To account for the discrete nature of magnitude data, the effective minimum magnitude was defined as [47]:

$$Mmin = Mc - \left(\frac{\Delta M}{2}\right) \tag{3}$$

where (Mc) is the magnitude of completeness and ΔM is the magnitude interval used in constructing the frequency–magnitude distribution. Consequently, the b-value can be expressed as [46]:

$$b = \frac{loge}{\overline{M} - (Mc - \frac{\Delta M}{2})} \tag{4}$$

This formulation was applied to the selected earthquake populations to estimate the overall and spatially variable b-values. The statistical significance of variations in b-value was evaluated by considering the uncertainty associated with each estimate rather than interpreting differences in b-value solely on the basis of their absolute magnitude. The uncertainty of the b-value was estimated using [42]:

$$\delta b = 2.30 b^2 \sqrt{\frac{\sum_{i=1}^{n} (M_i - \overline{M})^2}{n(n-1)}} \tag{5}$$

where (Mi) is the magnitude of the (i)-th earthquake, $\overline{M}$ is the mean magnitude of the selected earthquake population, (n) is the number of earthquakes used in the calculation, and δb represents the estimated uncertainty of the b-value. The uncertainty was considered when comparing b-values among different spatial regions, time periods, and focal-depth ranges.

Spatial variations in earthquake occurrence and b-value were investigated using Geographic Information System (GIS 10.8) techniques and ZMAP7 [39, 48]. The earthquake epicenters and hypocenters were mapped to examine their spatial relationship with the principal tectonic structures of the study region, including the Central Badakhshan Fault Zone and the Darvaz fault system. The spatial distribution of b-values was subsequently evaluated to identify areas characterized by relatively high and low b-values. For this purpose, b-values were calculated on a grid of 925 cells with a spacing of 5.8 km, and a minimum of 50 events above the magnitude of completeness (Mc) was specified for each grid cell. The calculated b-values varied approximately from 0.8 to 2.2, Figure 4(a) while the associated standard deviations ranged from approximately 0.05 to 0.35 Figure 4(b). The spatial b-value analysis was used to characterize variations in the frequency–magnitude distribution across the study area.

Temporal variations in b-value Figure 5(d) were also investigated to assess changes in the frequency–magnitude characteristics of earthquake occurrence through time [49]. For this purpose, a fixed-event sliding window of 50 earthquakes with a step of 15 events was used. Particular attention was given to periods associated with relatively large earthquakes, including the Mw 6.4 earthquake of 27 March 2002 Figure 5(a) and the Mw 6.6 earthquake of 8 August 2019 Figure 5(b). Temporal b-value variations were examined to identify changes in the proportion of small- and large-magnitude earthquakes before and after significant seismic activity [50]. The results were interpreted together with the temporal variation in catalogue completeness to distinguish potential seismicity-related changes from variations caused by changes in earthquake detection capability Figure 5 [43].

The dependence of b-value on focal depth was investigated by examining the frequency–magnitude distribution of earthquakes at different hypocentral depths[27, 46]. This analysis was used to characterize the vertical variation of earthquake occurrence within the study region and to identify depth intervals associated with relatively low or high b-values Figure 7(a). Particular variations were observed at depths of approximately 11.2, 34, and 226 km Figure 7. These depth-dependent variations were evaluated together with their associated b-value uncertainties and the distribution of earthquake magnitudes at the corresponding depths.

In addition to the b-value analysis, cumulative seismic moment was calculated to quantify the contribution of earthquakes of different magnitudes to the total seismic moment released during the study period Figure 6. Seismic moment (M_0) was estimated from moment magnitude using the standard relationship [51]**:**

$$log_{10} M_0 = 1.5Mw + 9.1 \tag{6}$$

where (M_0) is expressed in N·m. The cumulative seismic moment was then calculated as:

$$M_{0,cum}(t) = \sum_{i=1}^{n(t)} M_0, i \tag{7}$$

where M_0, i is the seismic moment of the (i)-th earthquake and n(t) represents the number of earthquakes occurring up to time (t). This analysis provides a quantitative measure of the cumulative seismic moment contribution of the earthquake population and emphasizes the dominant contribution of relatively large earthquakes to the total seismic moment.

The earthquake catalogue was processed and analyzed with the ZMAP7 toolbox implemented in MATLAB R2022b [39], which was employed for catalogue processing, magnitude-of-completeness estimation, Gutenberg–Richter analysis, b-value calculation, and spatial and temporal statistical analyses [32, 52]. GIS 10.8 techniques were used to prepare spatial maps and examine the distribution of earthquake epicenters, focal depths, b-values, and their relationships with the major tectonic structures of the study area [10]. The overall analytical procedure consisted of catalogue compilation and quality control, removal of duplicate and incomplete records, magnitude homogenization, estimation of catalogue

completeness, declustering, Gutenberg–Richter analysis, maximum-likelihood b-value estimation, uncertainty analysis, spatial and temporal b-value analysis, depth-dependent analysis, and cumulative seismic moment calculation [42, 46].

3. Results

The statistical analysis of the earthquake catalogue reveals clear spatial and temporal variations in earthquake occurrence, magnitude–frequency distribution, catalogue completeness, b-value, seismic moment release, and earthquake depth across Takhar Province and the surrounding region. The results presented in this section are based on the homogenized earthquake catalogue and the statistical procedures described in the Data and Methods section.

The final earthquake catalogue contains approximately 5076 recorded events covering the period from 1926 to 2025 Figure (1b). The magnitude–frequency distribution follows the Gutenberg–Richter relationship over the magnitude range in which the catalogue is considered complete Figure (2a). The number of earthquakes decreases systematically with increasing magnitude, indicating that small- to moderate-magnitude earthquakes constitute the majority of the recorded seismicity, whereas earthquakes with larger magnitudes occur less frequently.

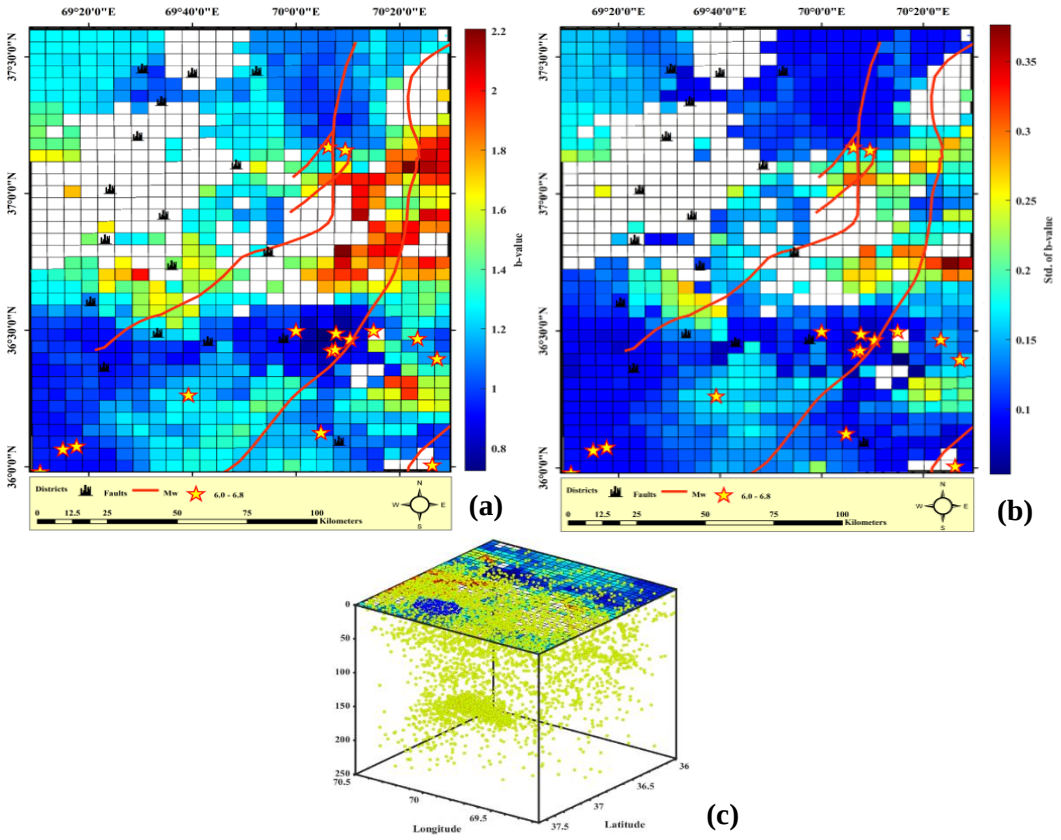


Figure 4. Spatial distribution of b-values and Standard deviation of b-values in Takhar Province. (a) b-value map showing spatial variations across the region. (b) Standard deviation map of b-values showing the reliability of b-value estimates. (c) **(c)** Three-dimensional distribution of the seismicity catalog and spatial b-values.

The magnitude of completeness, Mc, exhibits temporal variations throughout the study period Figure 3. During approximately 1926–1995, the estimated (Mc) is relatively high, with values of about 5.0–5.1. After 2000, the completeness magnitude generally decreases and shows greater temporal variability. This pattern is consistent with changes in earthquake detection capability and improvements in regional and global seismic monitoring networks. The temporal variation in Mc indicates that the completeness of the earthquake catalogue is not uniform throughout the entire study period. Therefore, comparisons of earthquake occurrence and b-values between different time intervals should take these variations in catalogue completeness into account, and the temporal variations in Mc should be considered when interpreting the long-term seismicity trends [53–55].

The spatial distribution of b-values shows heterogeneity across Takhar Province and the surrounding region Figure (4a). The estimated b-values range approximately from 0.8 to 2.2, while the associated standard deviations Figure (4b) generally range from about 0.05 to 0.35. Higher b-values occur in several localized areas, whereas relatively lower b-values are concentrated in specific parts of the study region. This spatial variability indicates that the earthquake magnitude–frequency distribution is not uniform throughout the study area. Areas characterized by relatively low b-values contain a comparatively larger proportion of moderate- to high-magnitude earthquakes than areas characterized by higher b-values. However, the spatial pattern of b-values should be interpreted together with the associated uncertainties and the spatial and temporal variations in catalogue completeness.

The b-value also exhibits considerable temporal variability during the study period Figure 5. Periods of relatively high and low b-values alternate through time, and no uniform temporal trend is observed [55]. Several variations occur during periods associated with relatively larger earthquakes. For the earthquake sequence associated with the Mw 6.4 event of 27 March 2002 Figure (5b), the estimated b-value is approximately 1.26 ± 0.20. For the Mw 6.6 earthquake that occurred on 8 August 2019 Figure 5(a) at a depth of approximately 220 km, the estimated b-value is approximately 1.60 ± 0.30. During the period from October 2019 to October 2020 Figure (5c), the estimated b-value is approximately 1.40 ± 0.30. These results indicate that the b-value varies through time and that periods associated with larger earthquakes may coincide with fluctuations

in the earthquake magnitude–frequency distribution. However, the observed temporal variations in b-value alone do not establish a deterministic relationship between b-value changes and the occurrence of individual earthquakes [49].

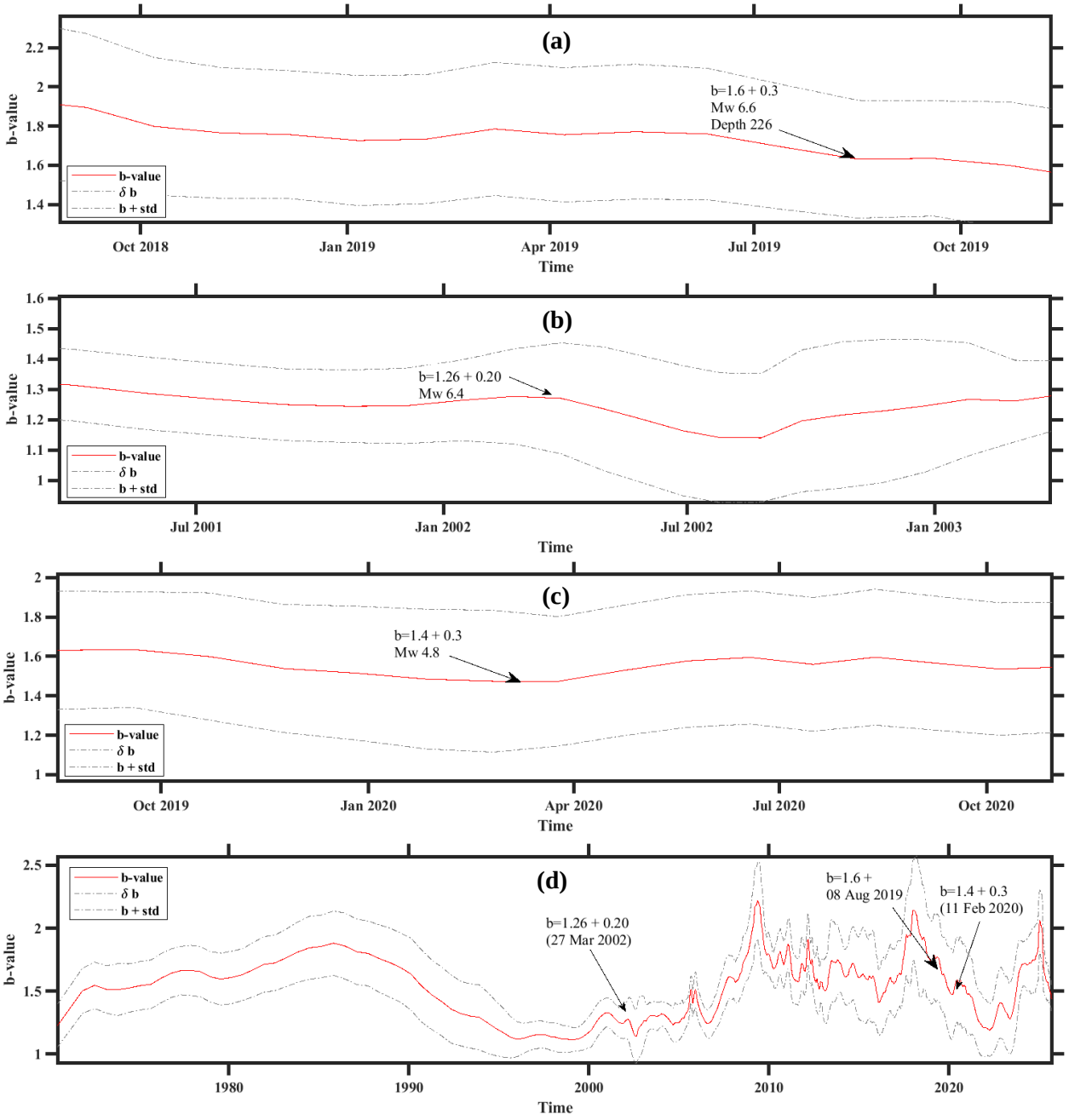


Figure 5. Graphs showing temporal variations of b-value for major earthquake sequences in Takhar Province. **(a)** b-value evolution around the Mw 6.6 event (depth 220 km) with b=1.6±0.3. on 08 Aug 2019. **(b)** b-value changes during the Mw 6.4 earthquake sequence on 27 Mar 2002 with b=1.26±0.20. **(c)** Temporal b-value variation around the Mw 4.8 event from Oct 2019 to Oct 2020 showing b=1.4±0.3. **(d)** Long-term b-value evolution in Takhar Province from 1926 to 2025.

The cumulative seismic moment release calculated from the homogenized moment magnitudes shows a strongly uneven temporal distribution Figure 6. The cumulative curves represent the progressive release of seismic moment recorded in the catalogue and do not imply the accumulation of tectonic strain. Most of the cumulative seismic moment is released during a relatively small number of moderate- to large-magnitude earthquakes, whereas the numerous smaller earthquakes contribute comparatively little to the total seismic moment. Several increases in cumulative seismic moment release are associated with larger earthquakes in the catalogue. The estimated seismic moments include approximately 0.09×10^{22} Nm for the July 1990 event, 0.52×10^{21} Nm for the 6 July 1962 event, 0.29×10^{21} Nm for the 23 April 1962 event, 0.12×10^{22} Nm for the 27 March 2002 event, 0.15×10^{22} Nm for the 8 August 2019 event, 0.17×10^{22} Nm for the 11 February 2020 event Figure 6(d).

The cumulative seismic-moment release curve indicates that seismic moment release is episodic rather than uniform through time (Figure 6d). Individual moderate- to large-magnitude earthquakes can produce abrupt increases in cumulative seismic moment release compared with the relatively gradual contribution of smaller events. The temporal pattern of seismic moment release is therefore strongly influenced by a limited number of larger earthquakes [10]. The relationship between earthquake depth, magnitude, and b-value reveals additional vertical heterogeneity in the seismicity distribution Figure (7d). Figure (7d) was generated by calculating the b-value for successive magnitude subsets

of the catalogue and is not interpreted as a b-value belonging to an individual magnitude. Several localized reductions in the estimated b-value occur at different depths. In particular, variations are observed near depths of approximately 11.2 km and 34 km Figure (7b) and Figure (7c), associated with earthquakes of (Mw 6.4) and (Mw 5.3), respectively. Another larger earthquake, with a magnitude of (Mw 6.6), occurred at a depth of approximately 226 km Figure (7a).

The occurrence of earthquakes at both shallow and intermediate depths indicates that the seismicity of the study region is not confined to a single depth interval. The observed variations in b-value with depth suggest that the earthquake magnitude–frequency distribution changes vertically within the study area. These variations are interpreted in terms of observed depth ranges rather than exact hypocentral depths, given the inherent uncertainties in earthquake depth determination. However, the statistical significance of individual depth-related b-value minima depends on the number of earthquakes included in each depth interval and on the corresponding uncertainty of the estimates. Overall, the results indicate spatial and temporal indicate in earthquake occurrence, catalogue completeness, b-value, seismic moment release, and earthquake depth in Takhar Province and the surrounding region. The spatial and temporal variations in b-value, together with the distribution of seismic moment release and earthquake depths, provide the statistical basis for further interpretation of the seismicity patterns and their possible relationship with the regional tectonic setting in the Discussion section.

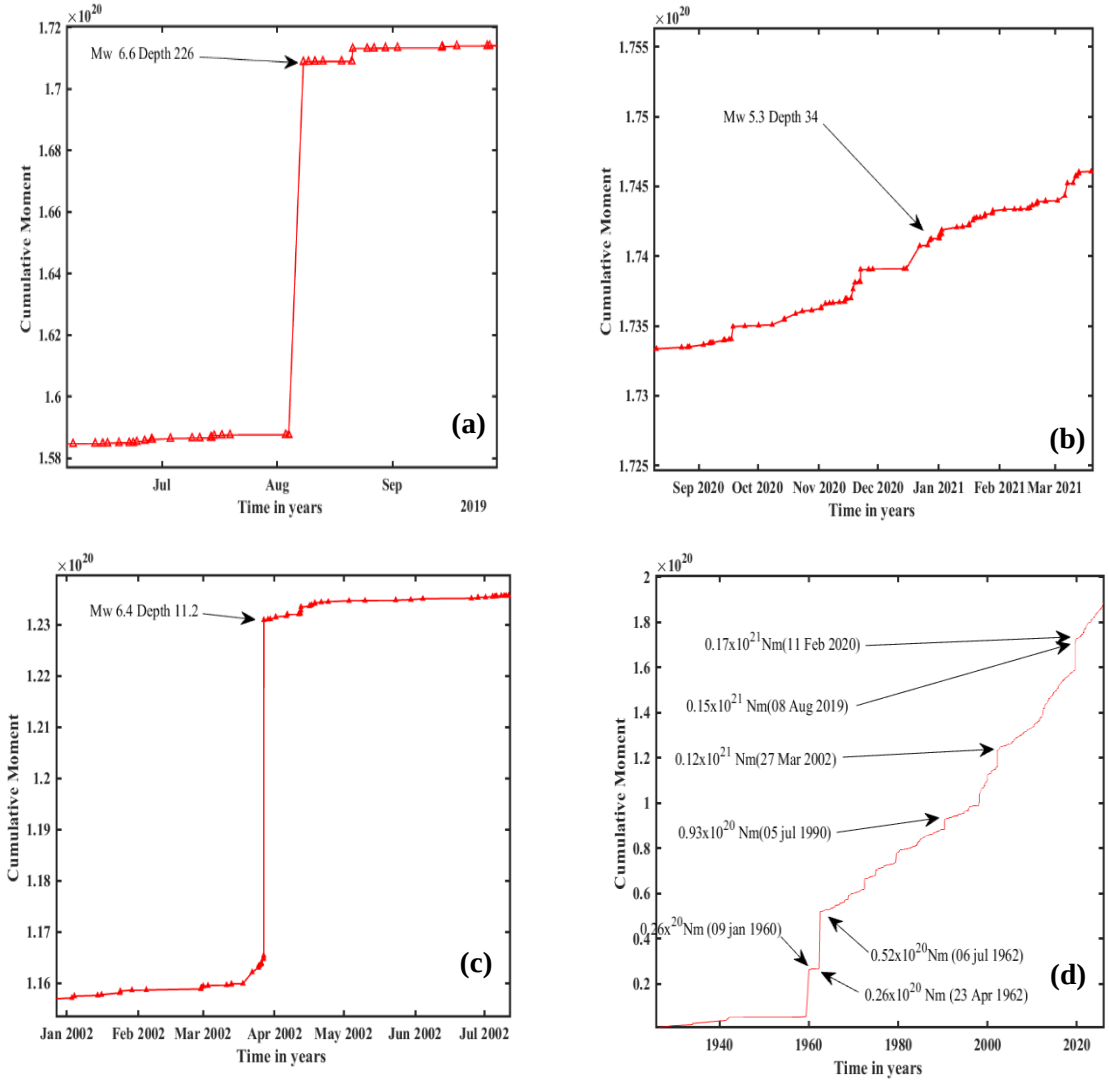


Figure 6. Graphs showing cumulative seismic moment release for individual major earthquakes in Takhar Province. (a) Cumulative moment for the Mw 6.6 event (depth 220 km) 08 Aug 2019. (b) Cumulative moment for the Mw 5.3 event (depth 34 km) from Sep 2020 to Mar 2021. (c) Cumulative moment for the Mw 6.4 event (depth 11.2 km) from Jan 2002 to Jul 2002. (d) Long-term cumulative moment from 1926 to 2025.

4. Discussion

The seismicity characteristics of Takhar Province indicate heterogeneity in earthquake occurrence across magnitude, time, space, and depth within the broader Hindu Kush–Pamir tectonic system. The overall b-value of 1.18 ± 0.02. indicates a predominance of small- to moderate-magnitude earthquakes (Figure 2a). Although slightly higher than the commonly adopted global reference value of approximately 1.0, this value remains within the range reported for tectonically active regions and is consistent with the general seismic characteristics of the Hindu Kush–Pamir region.

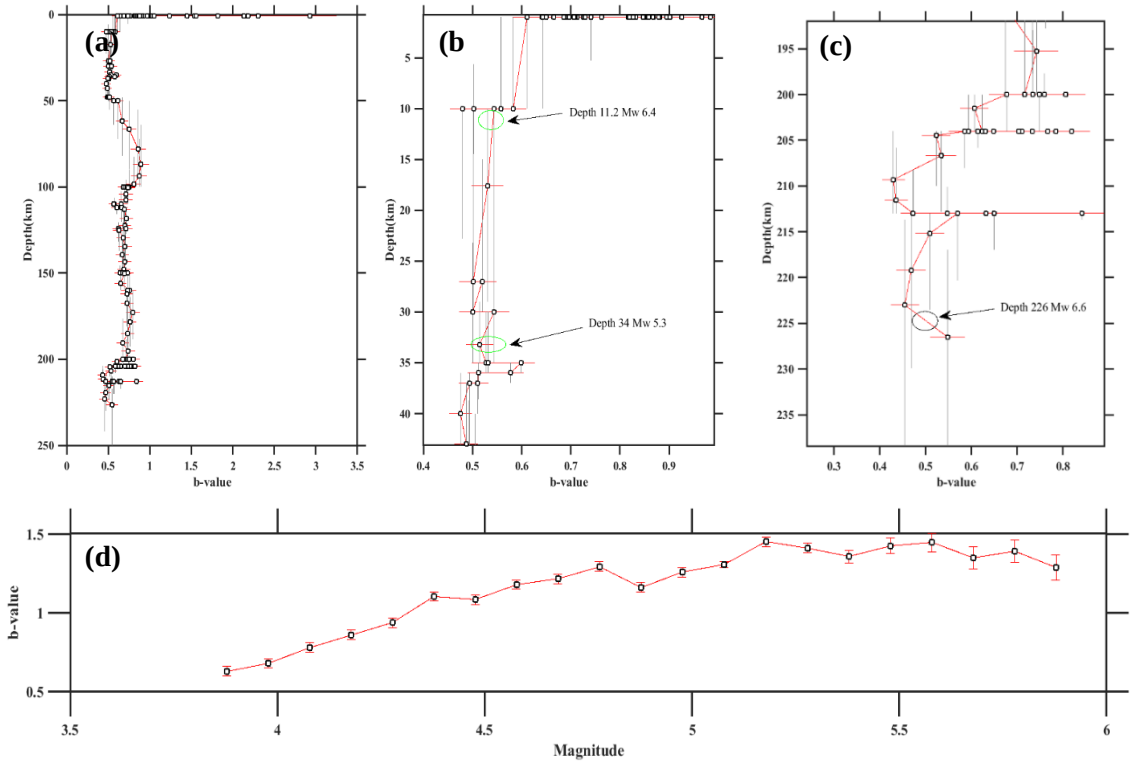


Figure 7. Variation of b-value with focal depth and moment magnitude (Mw), with associated uncertainty bars. (a) Overall b-value trend with depth down to 250 km. (b) b-value vs. depth in the shallow crust; two events at 11.2 km (Mw 6.4) and 34 km (Mw 5.3) are circled, marking notable b-value drops. **(c)** Enlarged view of b-value variation between 195–235km depth; the event at 226 km (Mw 6.6) is circled. **(d)** b-value as a function of magnitude, showing a general increasing trend with Mw. Error bars represent the uncertainty in b-value estimates.

The magnitude–frequency relationship obtained for Takhar is broadly comparable with previous regional studies. Rehman et al. (2017) reported b-values of 1.06–1.32. for shallow earthquakes and 0.90–1.07. for intermediate-depth earthquakes in the Hindu Kush, indicating a dependence of earthquake-size distributions on depth [25]. The Takhar value of 1.18 ± 0.02. falls within the reported range for shallow seismicity. Similarly, K. Rehman et al., (2023) using a relocated catalogue covering the Pamir–Hindu Kush seismic zone during 1949–2018, obtained b-values between 0.99 and 1.47 across the Hindu Kush, South Pamir, Central Pamir, and North Pamir [56]. The Takhar value therefore lies well within the regional range and supports its interpretation as part of the heterogeneous seismic regime of the Hindu Kush–Pamir collision zone rather than as an isolated seismic domain.

Further evidence for regional variability is provided by Rahman and Rehman, (2023), who analysed 14,158 earthquakes from northern Pakistan and adjacent tectonic domains and reported b-values ranging from 0.73 to 1.89, with values of approximately 0.5–2.5 in the Hindu Kush [57]. The spatial range identified in Takhar (approximately 0.8–2.2) (Figure 4a) is broadly consistent with this regional variability. Differences in the extent of the study areas, catalogue characteristics, and estimation procedures may explain variations in the numerical ranges among studies.

An important result of the present study is that b-value varies in both space and depth. The spatial distribution indicates differences among parts of Takhar, while localized reductions in b-value occur around approximately 11.2, 34, and 226 km depth Figure 7. These observations indicate that earthquake-size distributions are not uniform throughout the seismogenic volume. However, these variations are interpreted descriptively, since no formal statistical test was applied and the uncertainties of the b-value estimates should be considered. Singh and Singh (2015), using one- and two-dimensional b-value analyses beneath the Pamir–Hindu Kush region, identified significant depth-dependent variations in b-value[27]. These variations were interpreted in relation to changes in the physical properties of the subducting lithosphere, including possible effects of dehydration, temperature, and effective stress[27]. The underlying earthquake catalog was derived from the local seismic dataset of Sippl et al. (2013), which revealed complex and heterogeneous deep seismic structures beneath the Pamir–Hindu Kush region [54]. The consistency between these observations suggests that the b-value variations observed in Takhar may partly reflect heterogeneous seismic and lithospheric conditions.

However, the low-b-value zones should not be interpreted as direct measurements of stress. The b-value is sensitive to catalogue completeness, the number of earthquakes available for analysis, magnitude uncertainty, earthquake clustering, and the spatial and temporal dimensions of the sampling window [58, 59]. Consequently, the relatively low values identified around 11.2, 34, and 226 km Figure 5 are more appropriately regarded as statistical indicators of heterogeneous seismic conditions rather than direct evidence of elevated stress. Independent geological and geophysical observations are required to establish their physical origin[13, 54].

The occurrence of the Mw 6.6 earthquake at approximately 220–226 km depth Figure 7 on 8 August 2019 is particularly important for understanding the vertical structure of seismicity in the region. This intermediate- to deep-focus event indicates that earthquake deformation extends below the shallow crust. The coexistence of shallow and deep earthquakes, together with the observed depth-dependent b-value variations, indicates a vertically heterogeneous deformation regime in which earthquake-generating processes may differ between shallow crustal and deeper lithospheric environments Figure 7.

The temporal behaviour of seismicity provides an additional dimension to this heterogeneity. The 1926–2025 earthquake catalogue shows substantial fluctuations in earthquake occurrence, with relatively quiet periods interrupted by episodes of enhanced seismic activity. The temporal b-value also varies among individual seismic sequences. For example, the Mw 6.6 earthquake of 8 August 2019, at approximately 220 km depth, is associated with a b-value of 1.6 ± 0.3, whereas the Mw 6.4 sequence of 27 March 2002 has a value of 1.26 ± 0.20. Figure 5. The sequence associated with Mw 4.8 earthquakes during October 2019–October 2020 yields a b-value of approximately 1.4 ± 0.3. These variations

indicate that the statistical characteristics of earthquake occurrence can change through time and that seismicity in Takhar is episodic rather than temporally uniform.

The temporal behaviour is also reflected in the cumulative seismic moment Figure 6. Abrupt increases in cumulative moment associated with the Mw 6.4 event in March 2002 and the Mw 6.6 event in August 2019 indicate episodes of rapid seismic energy release. In contrast, the more gradual increases observed during other periods suggest a more gradual, progressive release of seismic moment. The cumulative curves represent the seismic moment released by the earthquakes recorded in the catalogue and do not imply the accumulation of tectonic strain. Taken together, the temporal b-value and cumulative-moment patterns indicate that seismicity in Takhar cannot be adequately described using a temporally invariant model.

The relationship between b-value and earthquake magnitude should nevertheless be interpreted cautiously. Although relatively low b-values may occur in association with periods or areas containing larger earthquakes, b-value alone cannot determine the timing or magnitude of future earthquakes. It is a statistical parameter describing the relative proportion of earthquakes of different magnitudes within a specified spatial and temporal population. Therefore, the low-b-value anomalies identified in Takhar should not be regarded as deterministic earthquake precursors. Their principal value lies in identifying areas and periods with distinct statistical characteristics of seismicity that may warrant further investigation in the context of seismic-hazard assessment.

Methodological differences among earthquake catalogues may also contribute to discrepancies between the present results and previous studies. Catalogue duration, magnitude scale, magnitude of completeness (Mc), hypocentral accuracy, spatial sampling, earthquake clustering, and statistical estimation procedures can all influence the calculated b-value. Such differences are particularly important when comparing the localized Takhar catalogue with regional datasets covering the entire Hindu Kush–Pamir system or northern Pakistan. Numerical comparisons should therefore be interpreted in relation to the characteristics and limitations of each catalogue.

Catalogue completeness is especially important when evaluating temporal variations. Changes in seismic-network detection capability through time can modify the minimum magnitude of earthquakes that can be reliably identified. Apparent temporal changes in earthquake frequency or b-value may consequently reflect changes in Mc rather than genuine variations in the underlying seismic process. This limitation is particularly relevant to the 1926–2025 catalogue because early instrumental coverage was considerably less developed than modern seismic monitoring. Temporal b-value variations should therefore be interpreted within the periods for which catalogue completeness is adequately constrained.

The observed spatial and depth-dependent patterns are also consistent with the complex tectonic setting of Takhar, which lies within the broader deformation zone associated with the India–Eurasia collision and the Hindu Kush–Pamir system. Variations in b-value may reflect differences in lithological properties, fault and fracture structures, stress conditions, and the geometry of active deformation at different depths. Nevertheless, a direct causal relationship between individual b-value anomalies and specific geological structures cannot be established from b-value analysis alone. Such interpretations would benefit from improved hypocentral locations, focal-mechanism solutions, seismic tomography, active-fault mapping, and geodetic observations.

Overall, the results indicate that Takhar Province is characterized by temporal, spatial, and depth-dependent heterogeneity in seismicity. The overall b-value of 1.18 ± 0.02. is Figure 2(a) consistent with the broader Hindu Kush–Pamir seismic regime, while its local variations indicate differences in earthquake-size distributions across both geographic and depth domains. The temporal fluctuations in earthquake occurrence, variations in b-value among major seismic sequences, and episodic changes in cumulative seismic moment further demonstrate that seismicity is not stationary through time. Together, these observations indicate that the seismic behaviour of Takhar reflects a complex and heterogeneous deformation system extending from the shallow crust to intermediate and deep lithospheric levels. Integrating b-value analysis with temporal seismicity patterns, earthquake depth, cumulative seismic moment release, improved earthquake catalogues, focal mechanisms, geodetic observations, and regional tectonic information can provide a more comprehensive basis for understanding the processes governing earthquake generation and for improving seismic-hazard assessment in the Hindu Kush–Pamir region.

5. Conclusion

This study provides an integrated assessment of seismicity in Takhar Province and its surrounding region using 5,076 earthquakes recorded between 1926 and 2025. The results indicate temporal, spatial, and depth-dependent heterogeneity in earthquake occurrence. The overall b-value of 1.18 ± 0.02, with a magnitude of completeness (Mc) of approximately 4.6, indicates a predominance of small- to moderate-magnitude earthquakes and is broadly consistent with the seismic characteristics of the wider Hindu Kush–Pamir region.

Spatially, b-values range from approximately 0.8 to 2.2, indicating substantial variations in earthquake-size distribution across the study area, with relatively low values identified in Ashkamish, Namak Ab, Bangi, Chiab, and Khawaja Bahawaldin. Temporally, the 1926–2025 seismicity is distinctly non-uniform, with relatively quiet intervals interrupted by episodes of enhanced activity. Variations in b-value among major seismic sequences suggest that the statistical characteristics of seismicity vary through time.

The cumulative seismic moment release also shows pronounced temporal changes, including abrupt increases associated with the Mw 6.4 earthquake in 2002 and the Mw 6.6 earthquake in 2019. In addition, depth-dependent variations in b-value and the occurrence of the Mw 6.6 earthquake at approximately 220–226 km depth indicate that seismic deformation extends from shallow crustal levels to intermediate and deep lithospheric depths. These depths indicate observed depth ranges rather than exact hypocentral depths, given the inherent uncertainties in earthquake depth determination.

Overall, the combined temporal, spatial, and depth-dependent patterns indicate that Takhar represents a complex and heterogeneous seismic regime within the Hindu Kush–Pamir tectonic system. Although b-value variations provide useful statistical information for seismic-hazard assessment, they should not be interpreted as deterministic indicators of future large earthquakes. Integrating b-value analysis with improved earthquake locations, focal mechanisms, geodetic observations, seismic tomography, and active-fault information will be essential for better understanding earthquake-generating processes and refining seismic-hazard assessment in the region.

Author Contributions

H.H.: Conceptualization, Investigation, Data Curation, Software, Visualization, Writing – Original Draft, Writing – Review & Editing.

Funding

This research received no external funding.

Data Availability Statement

The dataset used in this study is available from the corresponding author upon reasonable request.

Conflict of Interest Statement

The author declares that there is no conflict of interest. They have no known competing financial interests or personal relationships that could have appeared to influence the work reported in this paper.

References

[1.] Ahadov B, Ozturk S. Spatial variations of fundamental seismotectonic parameters for the earthquake occurrences in the Eastern Mediterranean and Caucasus. *Nat Hazards* 2022; 111: 2177–2192.

[2.] Gutenberg B, Richter CF. Earthquake magnitude, intensity, energy, and acceleration. *Bull Seism Soc* 1942; 32: 63–191.

[3.] Kamer Y. Minimum sample size for detection of Gutenberg-Richter's b-value. *ArXiv Prepr ArXiv14101815*.

[4.] Utkucu M, Uzunca F, Durmuş H, et al. Seismicity of the Southern Marmara Region (Türkiye) before and after the August 17, 1999 İzmit earthquake. Epub ahead of print 21 October 2022. DOI: https://doi.org/10.33793/acperpro.05.02.734.

[5.] Akhundzadah NA. Earthquake Risk Severity and Urgent Need for Disaster Management in Afghanistan. *GeoHazards* 2025; 6: 9.

[6.] Copley A, Avouac J, Royer J. India-Asia collision and the Cenozoic slowdown of the Indian plate: Implications for the forces driving plate motions. *J Geophys Res Solid Earth* 2010; 115: 2009JB006634.

[7.] Singh S, Ghosh A. The role of crustal models in the dynamics of the India–Eurasia collision zone. *Geophys J Int* 2020; 223: 111–131.

[8.] Ruleman CA. Neotectonic inversion of the Hindu Kush-Pamir Mountain Region. *US Geol Surv Open-File* 2011; 32: 95–111.

[9.] Kufner S-K, Kakar N, Bezada M, et al. The Hindu Kush slab break-off as revealed by deep structure and crustal deformation. *Nat Commun* 2021; 12: 1685.

[10.] Molnar P, Bendick R. Seismic Moments of Intermediate-Depth Earthquakes Beneath the Hindu Kush: Active Stretching of a Blob of Sinking Thickened Mantle Lithosphere? *Tectonics* 2019; 38: 1651–1665.

[11.] Schneider FM, Yuan X, Schurr B, et al. The Crust in the Pamir: Insights From Receiver Functions. *J Geophys Res Solid Earth* 2019; 124: 9313–9331.

[12.] Ammirati J-B, Mackaman-Lofland C, Zeckra M, et al. Stress transmission along mid-crustal faults highlighted by the 2021 Mw 6.5 San Juan (Argentina) earthquake. *Sci Rep* 2022; 12: 17939.

[13.] Kufner S, Eken T, Tilmann F, et al. Seismic Anisotropy Beneath the Pamir and the Hindu Kush: Evidence for Contributions From Crust, Mantle Lithosphere, and Asthenosphere. *J Geophys Res Solid Earth*; 123. Epub ahead of print December 2018. DOI: 10.1029/2018JB015926.

[14.] Boyd OS, Mueller CS, Rukstales KS. Preliminary earthquake hazard map of Afghanistan. *US Geol Surv Open-File Rep* 2007; 2007: 1137.

[15.] Mohammadi K, Moghimi E, Zare M, et al. Tectonic Setting and Seismicity of the Badakhshan Region Afghanistan. *J Seismol Earthq Eng*; 23. Epub ahead of print May 2021. DOI: 10.48303/jsee.2023.1971397.1032.

[16.] Ambraseys N, Bilham R. Earthquakes in Afghanistan. *Seismol Res Lett* 2003; 74: 107–123.

[17.] Dewey RW. Seismicity of Afghanistan and vicinity. Epub ahead of print 2006. DOI: 10.3133/ofr20061185.

[18.] Scholz C. The frequency-magnitude relation of microfracturing in rock and its relation to earthquakes. *Bull Seismol Soc Am* 1968; 58: 399–415.

[19.] Scholz CH. On the stress dependence of the earthquake *b* value. *Geophys Res Lett* 2015; 42: 1399–1402.

[20.] Schorlemmer D, Wiemer S, Wyss M. Variations in earthquake-size distribution across different stress regimes. *Nature* 2005; 437: 539–542.

[21.] Leptokaropoulos KM, Karakostas VG, Papadimitriou EE, et al. A homogeneous earthquake catalog for Western Turkey and magnitude of completeness determination. *Bull Seismol Soc Am* 2013; 103: 2739–2751.

[22.] Mignan A, Woessner J. Estimating the magnitude of completeness for earthquake catalogs. *Community Online Resour Stat Seism Anal* 2012; 1–45.

[23.] Woessner J, Wiemer S. Assessing the quality of earthquake catalogues: Estimating the magnitude of completeness and its uncertainty. *Bull Seismol Soc Am* 2005; 95: 684–698.

[24.] Nicknam A, Mail E, Yazdani A. Applying b-value statistical variation to seismic hazard analysis. *INDIAN J MAR SCI*; 46.

[25.] Rehman K, Ali W, Ali A, et al. Shallow and intermediate depth earthquakes in the Hindu Kush region across the Afghan-Pakistan border. *J Asian Earth Sci* 2017; 148: 241–253.

[26.] Singh C. Spatial variation of seismic *b*- values across the NW Himalaya. *Geomat Nat Hazards Risk* 2016; 7: 522–530.

[27.] Singh C, Singh S. Imaging b-value variation beneath the Pamir-Hindu Kush region. *Bull Seismol Soc Am* 2015; 105: 808–815.

[28.] Ruff L, Kanamori H. Seismicity and the subduction process. *Phys Earth Planet Inter* 1980; 23: 240–252.

[29.] Gutenberg B, Richter CF. Frequency of earthquakes in California.

[30.] Pavlenko VA, Zavyalov AD. Comparative Analysis of the Methods for Estimating the Magnitude of Completeness of Earthquake Catalogs. 58.

[31.] Chen J, Zhu S. Spatial and temporal b-value precursors preceding the 2008 Wenchuan, China, earthquake (Mw = 7.9): implications for earthquake prediction. *Geomat Nat Hazards Risk* 2020; 11: 1196–1211.

[32.] Gong W, Chen H, Gao Y, et al. A test on methods for Mc estimation and spatial-temporal distribution of b-value in the eastern Tibetan Plateau. *Front Earth Sci* 2024; 12: 1335938.

[33.] Talbi A, Bellalem F, Mobarki M. Turkey and adjacent area seismicity forecasts from earthquake inter-event time mean ratio statistics. *J Seismol* 2019; 23: 441–453.

[34.] Iwata D, Nanjo KZ. Adaptive estimation of the Gutenberg–Richter b value using a state space model and particle filtering. *Sci Rep* 2024; 14: 4630.

[35.] International Seismological Centre. ISC Bulletin: Event Catalogue Search [Internet]. Thatcham, United Kingdom: International Seismological Centre. Available from: https://www.isc.ac.uk/iscbulletin/search/catalogue/.

[36.] U.S. Geological Survey. Search Earthquake Catalog [Internet]. Reston, VA: U.S. Geological Survey. Available from: https://earthquake.usgs.gov/earthquakes/search/.

[37.] Scordilis E. Empirical global relations converting MS and mb to moment magnitude. *J Seismol* 2006; 10: 225–236.

[38.] Ernandi FN. Analisis variasi a-value dan b-value dengan menggunakan software zmap v. 6 sebagai indikator potensi gempa bumi di wilayah Nusa Tenggara Barat. *Inov Fis Indones* 2020; 9: 24–30.

[39.] Wiemer S. A software package to analyze seismicity: ZMAP. *Seismol Res Lett* 2001; 72: 373–382.

[40.] Reasenberg PA. Second-order moment of central California seismicity, 1969–1982. *J Geophys Res* 1985; 90: 5479–5495.

[41.] Reasenberg PA. Foreshock occurrence before large earthquakes. 1999; 104: 4755–4768.

[42.] Shi Y, Bolt BA. The standard error of the magnitude-frequency b value. *Bull Seismol Soc Am* 1982; 72: 1677–1687.

[43.] Wiemer S. Minimum Magnitude of Completeness in Earthquake Catalogs: Examples from Alaska, the Western United States, and Japan. *Bull Seismol Soc Am* 2000; 90: 859–869.

[44.] Wyss M, Shimazaki K, Wiemer S. Mapping active magma chambers by *b* values beneath the off-Ito volcano, Japan. *J Geophys Res Solid Earth* 1997; 102: 20413–20422.

[45.] Dogru A. Seismic hazard assessment of the central North Anatolian Fault (Turkey) from GPSderived strain rates and b-values. *Geomat Nat Hazards Risk* 2018; 9: 356–367.

[46.] Aki K. Maximum likelihood estimate of b in the formula log N= a-bM and its confidence limits. *Bull Earthq Res Inst Tokyo Univ* 1965; 43: 237–239.

[47.] Chang Y, Wang R, Han P, et al. b-Value Evaluation and Applications to Seismic Hazard Assessment. *Entropy* 2025; 27: 958.

[48.] Zhao SJ, Xiong LY, Ren AZ. A Spatial–Temporal Stochastic Simulation of Fire Outbreaks Following Earthquake Based on GIS. *J Fire Sci* 2006; 24: 313–339.

[49.] Sarjan AFN. Spatiotemporal analysis of Seismicity Parameters (a-and b-values) for Earthquake Disaster Mitigation: A case study of the 2018 Lombok Earthquake, Indonesia. *Lambda J Ilm Pendidik MIPA Dan Apl* 2025; 5: 700–712.

[50.] Bellalem F, Mobarki M, Talbi A. Analysis of spatio-temporal seismic activity in Northern Algeria. 2008.

[51.] Hanks TC, Kanamori H. A moment magnitude scale. *J Geophys Res Solid Earth* 1979; 84: 2348–2350.

[52.] Kijko A, Smit A, Sellevoll MA. Estimation of Earthquake Hazard Parameters from Incomplete Data Files. Part III. Incorporation of Uncertainty of Earthquake-Occurrence Model. *Bull Seismol Soc Am* 2016; 106: 1210–1222.

[53.] Molnar P, Tapponnier P. Cenozoic Tectonics of Asia: Effects of a Continental Collision: Features of recent continental tectonics in Asia can be interpreted as results of the India-Eurasia collision. *Science* 1975; 189: 419–426.

[54.] Sippl C, Schurr B, Yuan X, et al. Geometry of the Pamir-Hindu Kush intermediate-depth earthquake zone from local seismic data. *J Geophys Res Solid Earth* 2013; 118: 1438–1457.

[55.] Yadav RBS, Tsapanos TM, Koravos GCh, et al. Spatial mapping of earthquake hazard parameters in the Hindukush–Pamir Himalaya and adjacent regions: Implication for future seismic hazard. *J Asian Earth Sci* 2013; 70–71: 115–124.

[56.] Rehman K, Ali W, Shafique M, et al. Variations of b-value and the ω-upper bound magnitude of GIII distribution of the Pamir–Hindu Kush region. Epub ahead of print 23 October 2023. DOI: 10.1007/s12517-023-11707-4.

[57.] Rahman Z, Rehman K. Seismic b value analysis of north Pakistan: an appraisal. Epub ahead of print 13 December 2023. DOI: 10.1007/s12665-023-11306-2.

[58.] Hisyam F, Susilo A, Anshori M, et al. Spatio-Temporal Variation Seismicity Pattern in East Java Between 2002 and 2022 Based on the b-value and Seismic Quiescence z-value. *Trends Sci* 2024; 21: 7608.

[59.] Wen F, Dong W, Xu F, et al. Spatial and temporal evolution of land use and habitat quality in arid regions – a case of Northwest China. *Open Geosci* 2025; 17: 20220695.

How to Cite This Article

Hawadi, H., Temporal, Spatial, and Depth-Dependent Seismicity of Takhar, Afghanistan: Insights from b-Value Variations and Seismic Moment Release, Civil Engineering Beyond Limits, 2(2027), 11196.
https://doi.org/10.36937/cebel.2027.11196